

# One-step real-time duplex reverse transcription PCR simultaneously quantify analyte and housekeeping gene mRNAs

Chengming Wang, Dongya Gao, Alexander Vaglenov, and Bernhard Kaltenboeck

*BioTechniques* 36:508-519 (March 2004)

*We developed a one-step real-time duplex reverse transcription PCR (RT-PCR) method using the LightCycler® platform. This method allows simultaneous reverse transcription and real-time PCR amplification of two mRNAs of specific genes of interest (analyte genes) and mRNA of constantly transcribed genes (housekeeping genes) in a single-tube reaction. Specimen total nucleic acids were used because eukaryotic cDNA is discriminated from genomic DNA using exon-spanning primers and/or fluorescence resonance energy transfer (FRET) probes. Transcripts of murine arginase I and hypoxanthine-phosphoribosyl transferase (HPRT; housekeeping gene) or murine arginase II analyte and porphobilinogen deaminase (PBGD; housekeeping gene) were quantified in such duplex RT-PCRs. Twenty-minute reverse transcription reactions at 55°C followed by 18 high-stringency step-down thermal cycles and 25 relaxed-stringency fluorescence acquisition cycles produced sensitive and accurate RT-PCR results. Fluorescent signal spillover between channels was fully compensated. A matrix of duplex PCRs at variable ratios of target standards yielded equations for factors that correct PCR-specific target ratio-dependent deviations in quantification. The one-step real-time duplex RT-PCRs reliably and accurately determined 10–10,000 copies of each target over a 100,000-fold range of target copy ratios (analyte to housekeeping mRNA = 10<sup>-2.5</sup>–10<sup>2.5</sup>) in a single assay.*

## INTRODUCTION

Of all methods used to quantify mRNA, real-time reverse transcription PCR (RT-PCR) is considered the most sensitive and accurate one (1). In addition to its wide use in laboratory research, real-time RT-PCR has the potential for broad application in the diagnoses of functional defects in disease. The absolute quantification of mRNA is generally impractical and unnecessary because constantly transcribed housekeeping genes effectively serve as internal standards for the relative quantification of the transcripts of genes of interest (1–5). Fluorescent probes in real-time PCR have remedied specificity problems inherent to the quantification of amplification products by double-stranded DNA-binding fluorescent dyes (2). Nevertheless, RT-PCR is still a cumbersome technique that requires multiple reactions per single specimen.

In many RT-PCR methods, genomic DNA must be removed to avoid false-positive amplification. The separation of reverse transcription and PCR into a two-step RT-PCR is necessary if multiple targets are to be quantified relative to housekeeping gene transcripts. Finally, one-step RT-PCR, which combines reverse transcription and amplification into one reaction, determines absolute, but not relative, amounts of single targets. These absolute quantities of different gene transcripts cannot be related to each other because variations in reverse transcription and amplification efficiency cannot be controlled between different single-target one-step RT-PCRs. Collectively, these limitations increase the sample size required for the reaction and decrease the sensitivity and specificity, thus preventing routine clinical diagnostic use of this powerful technique and rendering laboratory research applications cumbersome.

In this study, we combined two independent real-time PCR methods into a single reaction termed duplex PCR, which allows simultaneous amplification and quantification of transcripts of both an analyte and a housekeeping gene. We present data that indicate the validity of such a real-time duplex PCR method that also performs reverse transcription in this single reaction prior to amplification. The present study examines in detail the properties of one-step real-time duplex RT-PCR methods that remove major technical limitations of real-time RT-PCR.

## MATERIALS AND METHODS

### Extraction of Total Nucleic Acids and RNase Treatment

Macrophages elicited via intraperitoneal thioglycollate injection from male A/J and C57BL/6J mice were plated in

24-well plates stimulated with *Chlamydia pneumoniae* lysate and removed with a cell scraper (6). Total nucleic acids were extracted from sedimented cells using the High Pure<sup>®</sup> PCR Template Preparation Kit (Roche Applied Science, Indianapolis, IN, USA) as previously described and eluted in 10 mM Tris-HCl, pH 8.5, 0.1 mM EDTA (TE) (7). For selected analyses, RNA in total nucleic acids was hydrolyzed at 37°C for 30 min with DNase-free RNase (Invitrogen, Carlsbad, CA, USA) at 12.5 µg/mL. All experimental animal procedures utilized in this research followed the National Institutes of Health (Bethesda, MD, USA) guidelines and were reviewed and approved by the Auburn University Animal Care and Use Committee (Auburn, AL, USA).

### Design of Primers and Probes

Primers and fluorescence resonance energy transfer (FRET) probes were obtained from Qiagen (Valencia, CA, USA) and are shown in Table 1. Oligonucleotides were designed to span exon boundaries, thus allowing only amplification from, and detection of, cDNA but not genomic DNA. The lengths of the amplification products were between 160–220 bp. All oligonucleotides were designed using *Vector NTI*<sup>®</sup> software (InforMax, Frederick, MD, USA) for a calculated melting temperature ( $T_m$ ) of 71°–73°C, assuming a 190-mM salt concentration and a 100-pM oligonucleotide concentration. Carboxyfluorescein [6-carboxyfluorescein (6-FAM)] probes were 3' labeled and used unpurified as FRET energy donor probes excited by 488 nm light. BODIPY<sup>®</sup> 630/650 (Molecular Probes, Eugene, OR, USA) and Cy<sup>TM</sup>5.5 probes were 5'-labeled, 3'-phosphorylated, high-performance liquid chromatography (HPLC)-purified, and used as acceptor probes (8). Fluorescence emitted from BODIPY 630/650 probes served for the detection of the analyte gene arginase I and arginase II mRNAs (9–11) at 640 nm and from Cy5.5 probes for detection of the porphobilinogen deaminase (PBGD) and hypoxanthine-phosphoribosyl transferase (HPRT) housekeeping genes (3,4,5,12,13) at 705 nm in each duplex PCR (arginase I plus HPRT; arginase II plus PBGD).

### Reaction Mixture for One-Step Real-Time Duplex RT-PCR

The PCR buffer consisted of 20 mM Tris-HCl, pH 8.4, 50 mM KCl, 4.5 mM MgCl<sub>2</sub>, 0.05% Nonidet<sup>TM</sup> P-40, 0.05% Tween<sup>®</sup> 20, 0.03 % acetylated bovine serum albumin (BSA), and 200 µM each dATP, dCTP, dGTP, and 600 µM dUTP. Reactions were performed in glass capillaries with 15 µL of 1.33× master mixture and 5 µL of sample nucleic acids or standards. Each 20-µL reaction contained 2.0 U Platinum<sup>®</sup> *Taq* DNA polymerase (Invitrogen), 0.2 U heat-labile uracil-N-glycosylase (Roche Applied Science), and 0.0213 U ThermoScript<sup>TM</sup> reverse transcriptase (Invitrogen). PBGD primers were used at 0.8 µM, all other primers at 1 µM, BODIPY 630/650 and Cy5.5 probes at 0.2 µM, and 6-FAM probes at 0.1 µM. Master mixtures were prepared freshly from 10× PCR buffer, 5× oligonucleotide mixture, 50× nucleotide mixture, and enzymes. For convenient pipetting, ThermoScript reverse transcriptase was used at a 1:140 dilution in storage buffer. Standard reactions containing 10,000, 1000, 100, or 10 copies of each target were performed with each run.

### Thermal Cycling

All PCRs were performed on the LightCycler<sup>®</sup> Real-Time PCR Platform using LightCycler Software Version 3.5 (both from Roche Applied Science). Thermal cycling was preceded by a 20-min reverse transcription step at 55°C, followed by a 5-min incubation at 95°C. Thermal cycling consisted of 18 high-stringency step-down cycles followed by 25 relaxed-stringency fluorescence acquisition cycles. The 18 high-stringency step-down thermal cycles for the arginase I-HPRT duplex PCR were 6 cycles of 15 s at 95°C, 60 s at 75°C; 9 cycles of 15 s at 95°C, 60 s at 73°C; and 3 cycles of 15 s at 95°C, 30 s at 71°C, and 30 s at 72°C. The high-stringency step-down thermal cycles for the arginase II-PBGD duplex PCR were 6 cycles of 15 s at 95°C, 60 s at 72°C; 9 cycles of 15 s at 95°C, 30 s at 70°C, 30 s at 72°C; and 3 cycles of 15 s at 95°C, 30 s at 68°C, 30 s at 72°C. The relaxed-stringency fluorescence acquisition cycling for both duplex

**Table 1. Oligonucleotide Primers and Probes Used in this Study**

Primer/Probe	Sequence <sup>a</sup>	cDNA Base Pair Location	T <sub>m</sub> <sup>b</sup> (°C)	RT-PCR Product, Length, GenBank <sup>®</sup> Accession No.
muARG1UP	5'-GTGGAGACCACAGTCTGGCAGTTGGA-3'	372–397 exon 3, 4	72.6	Mouse Arginase I 212 bp BC 013341
muARG1DN	5'-GCAGGGAGTCACCCAGGAGAATCCT-3'	583–559 exon 5	71.9	
muARG1BOD	5'-BODIPY 630/650-GAAGGAACTGAAAGGAAAGTTCCCA-GATGT-Phos-3'	526–555 exon 4, 5	71.5	
muARG1FLU	5'-CATGGGCAACCTGTGTCCTTTCTCC-6-FAM-3'	500–524 exon 4	71.9	
muARG2UP	5'-TTTCTCTCGGGGACAGAAGAAGCTAGGA-3'	96–123 exon 1	72.0	Mouse Arginase II 160 bp BC 023349
muARG2DN	5'-CAGATTATTGTAGGGATCATCTTGTGGGACA-3'	255–225 exon 3	71.6	
muARG2BOD	5'-BODIPY 630/650-TCTTCAGCAAGCCAGCTTCTCGAATGG-Phos-3'	143–169 exon 2	72.8	
muARG2FLU	5'-GGTGGCATCCCAACCTGGAGAGC-6-FAM-3'	171–193 exon 2, 3	72.6	
muPBGDUP	5'-CGGCCACAACCGCGGAAGAA-3'	20–39 exon 1, 3	71.7	Mouse PBGD 164 bp M28663, M28664 M28665, M28666
muPBGDDN	5'-GTCTCCCGTGGTGGACATAGCAATGA-3'	183–158 exon 4, 5	73.0	
muPBGDCY5.5	5'-Cy5.5-TCGAATCACCCCTCATCTTTGAGCCGT-Phos-3'	90–68 exon 3, 4	72.1	
muPBGDFLU	5'-CAGCTGGCTCTTACGGGTGCCCA-6-FAM-3'	66–41 exon 3	71.0	
muHPRTUP	5'-TCCCAGCGTCGTGATTAGCGATGA-3'	102–125 exon 1, 2	72.7	Mouse HPRT 172 bp NM 013556
muHPRTDN	5'-AATGTGATGGCCTCCCATCTCCTTCATGACAT-3'	273–242 exon 3	72.9	
muHPRTCY5.5	5'-Cy5.5-GATTATGGACAGGACTGAAAGACTTGCTCG-Phos-3'	210–239 exon 2, 3	71.7	
muHPRTFLU	5'-GGATTTGGAAAAAGTGTATTTCCTCATGGAC-6-FAM-3'	177–208 exon 2	72.7	

T<sub>m</sub>, melting temperature; RT-PCR, reverse transcription PCR; PBGD, porphobilinogen deaminase; HPRT, hypoxanthine-phosphoribosyl transferase.  
<sup>a</sup>BODIPY 630/650, amine-reactive BODIPY fluorophore attached to the 5' terminus; Cy5.5, cyanoethyl phosphoramidite attached to the 5' terminus; 6-FAM, 6-carboxyfluorescein attached to 3'-O-ribose; Phos, phosphate group attached to the 3' terminus.  
<sup>b</sup>The T<sub>m</sub> was calculated for a 190-mM salt concentration and a 100-pM probe concentration.

PCRs consisted of 25 cycles of 15 s at 95°C, 8 s at 58°C, followed by fluorescence acquisition, then 30 s at 65°C, and 30 s at 72°C.

Single-target (simplex) PCRs for arginase I, arginase II, HPRT, and PBGD used a lower Platinum *Taq* DNA polymerase quantity of 1.5 U/20 µL reaction, but otherwise identical protocols. *C. pneumoniae* 23S rRNA FRET real-time PCR was performed as previously described (7).

All types of duplex PCR were analyzed by agarose gel electrophoresis, the presence of two correctly sized am-

plification products and absence of aberrant products were verified, and both amplification products of each duplex PCR were DNA-sequenced.

**Color Compensation**

A color compensation file was created in a calibration cycling protocol with 4 samples in PCR buffer without enzymes (sample 1, blank; 2, 1 µM fluorescein probe; 3, 1 µM BODIPY 630/650 probe; 4, 1 µM Cy5.5 probe). The thermal cycling protocol for the calibration of color compensation was 30 s at 95°C; 40

cycles of 0 s at 95°C, 10 s at 55°C, 10 s at 72°C, and 1 temperature gradient step from 5 s at 40°C to 0 s at 95°C, followed by 30 s at 40°C. After calibration cycling, data were saved as color compensation files and imported for the analysis of the duplex RT-PCR data.

**PCR Standards**

Templates for standard reactions were prepared from RT-PCRs that contained 200 µM dTTP instead of dUTP. This rendered the standards insensitive to cleavage by uracil-N-gly-

cosylase, which was used to prevent PCR product carryover. PCR products were isolated by 4% MetaPhor<sup>®</sup> agarose gel electrophoresis (Cambrex, Rockland, ME, USA), extracted by glass matrix binding and elution, quantified by PicoGreen<sup>®</sup> DNA fluorescence assays (Molecular Probes), verified by DNA sequencing, and used at 10<sup>4</sup>, 10<sup>3</sup>, 10<sup>2</sup>, 10, and 0 copies per 5  $\mu$ L in a background of 100 ng purified pGEM<sup>®</sup> plasmid DNA (Promega, Madison, WI, USA) in TE.

For evaluation of the quantification of the duplex PCR standards at different target ratios and concentrations, each of 10<sup>4</sup>, 10<sup>3</sup>, 10<sup>2</sup>, or 10 copies of analyte standards (arginase I and arginase II) were combined with each of 10<sup>4</sup>, 10<sup>3</sup>, 10<sup>2</sup>, or 10 copies of housekeeping gene standards (HPRT or PBGD), and each combination was quantified in duplicate in two independent duplex PCRs. The copy numbers of each target in relation to the copies of the other respective target as found in the assays were determined, related to actual standard copy numbers, and equations for correction factors were deduced by linear least-square regression analysis (STATISTICA 6.1 software; StatSoft, Tulsa, OK, USA). For the analysis of samples by duplex RT-PCR, standard reactions containing 10<sup>4</sup>, 10<sup>3</sup>, 10<sup>2</sup>, or 10 copies of both DNA templates were performed without reverse transcription and used to quantify the concentrations of specimen mRNAs, which had been subjected to reverse transcription. The negative control was 100 ng purified pGEM plasmid DNA in 5  $\mu$ L TE, and mouse macrophage total nucleic acid that is positive for the respective targets served as the control for reverse transcription.

## RESULTS

Prior to characterizing the one-step real-time duplex RT-PCR assays, we undertook extensive efforts to optimize the methodology, starting from previously established reaction chemistries and step-down thermal cycling (7,14). Concentrations of reverse transcriptase, *Taq* DNA polymerase, primers, and all steps in the thermal cycling protocols were calibrated. Of particular importance for fine-tuning the reactions were

the amount of reverse transcriptase, the relative numbers and annealing temperatures of high-stringency step-down cycles (beginning at 70°–75°C), and the relaxed-stringency fluorescence acquisition cycles including fluorescence acquisition at 58°C after 8 s equilibration followed by 30 s annealing at 63°–65°C (data not shown). For all duplex RT-PCRs, agarose gel electrophoresis demonstrated correct amplification products, and the DNA sequencing results of the amplified fragments precisely matched the mRNA sequences.

### Specificity of One-Step Real-Time Duplex RT-PCR

To evaluate the ability of the one-step RT-PCRs to discriminate between genomic DNA and mRNA targets, we amplified total nucleic acids isolated from mouse macrophages stimulated with lysed *C. pneumoniae* bacteria. Sample nucleic acids were or were not treated with RNase and were amplified in the presence or absence of reverse transcriptase. Only *C. pneumoniae* DNA, but not the four mRNA targets, were amplified in the absence of reverse transcriptase (data not shown). The RNase treatment of total nucleic acids abolished the amplification of the mRNA targets but not of the *C. pneumoniae* DNA. These results validated the application of the one-step RT-PCR using exon-spanning primers and probes to the analysis of total nucleic acid specimens.

### Evaluation of Target Quantification

DNA standards containing equal amounts of both targets had served to establish one-step real-time duplex RT-PCR. A fundamental question in duplex PCR is how the targets interact during amplification and fluorescence detection when they are present in unequal ratios. To examine these interactions, we performed for each of the four possible pairs of analyte (arginase I and arginase II) and housekeeping genes (HPRT and PBGD) a matrix of standard duplex reactions in the absence of reverse transcriptase in which 10<sup>4</sup>, 10<sup>3</sup>, 10<sup>2</sup>, or 10 copies of one target were combined with 10<sup>4</sup>, 10<sup>3</sup>, 10<sup>2</sup>, or

10 copies of the other respective target. Figure 1 shows as an example the results for the arginase II-PBGD duplex PCR. These reactions, termed standard performance, demonstrated that targets in approximately 300-fold or lower abundance than the other target in a duplex PCR were amplified less efficiently and underreported (Figure 1). This was true for all targets in all combinations, but varied depending on thermal cycling conditions. In the final protocols, we adjusted the thermal cycling parameters so that amplification of the analyte genes was more efficient than that of the housekeeping genes (as evident in Figure 1 and Figure 2, plots A and C) for arginase II in comparison to PBGD. The rationale for this approach was that the highest sensitivity for the amplification of housekeeping gene mRNA was unnecessary because a minimum of 20–30 copies of housekeeping gene mRNA is required for accurate normalization. Thus, copy numbers of housekeeping gene mRNAs lower than 20, even if quantified precisely, would still not allow the accurate determination of analyte mRNA copies, which presumably will show a wider concentration range than housekeeping gene mRNA.

To evaluate the relative shifts in amplification efficiencies and data reporting, we plotted for each duplex PCR the results of two replicates of duplicate reactions as the logarithm of target ratio determined in the assay versus the ratio of actual to assay-determined targets. The equation for the least-square best fit regression line allows for the determination of an assay-specific correction factor for each target and its ratio to the other respective target. The data plotted for the arginase II-PBGD duplex PCR in Figure 2 clearly indicate for both analyte and housekeeping gene targets a reduced amplification efficiency at low abundance ( $\log$  target ratio  $< 0$ ; correction factors  $> 1$ ) and increased efficiency at high abundance ( $\log$  target ratio  $> 0$ ; correction factors  $\leq 1$ ). For PBGD, the correction factor at  $-2.5$ , which is the lowest acceptable logarithm of target ratios, is higher than that of arginase II (1.238 vs. 1.168), reflecting the adjustment of thermal PCR parameters in favor of the analyte arginase II. Similar relationships between correction factors and target ratios were found for the arginase I-HPRT duplex PCR. Plots of logarithm actual target copies versus logarithm assay-determined corrected target copies in Figure 2 reveal linear

fits with narrow confidence intervals over the 3-log range of the standard targets tested. These corrected assay data of all duplex PCRs correlated better with actual copy numbers than the uncorrected assay results (data not shown). It is important to notice that only log target ratios between  $-2.5$ – $2.5$  were used to calculate the correction factors. Higher and lower values were excluded because of the assay inaccuracy for the respective lower target. Therefore, the duplex PCRs as described allow the reliable determination of 10–10,000 copies of each target over a 100,000-fold range ( $10^{-2.5}$ – $10^{2.5}$ ; equal to 1/320 to 320) of the target copy ratios.

### Color Compensation

The LightCycler Real-Time PCR Platform acquires fluorescent signals in FRET duplex PCR at three emission wavelengths, and residual signal of short wavelength peaks may obscure fluorescence peaks in the long wavelength channels. To compensate for such fluorescence spillover, we acquired signals for a color compensation file according to the LightCycler instructions and used this file to electronically compensate for fluorescence

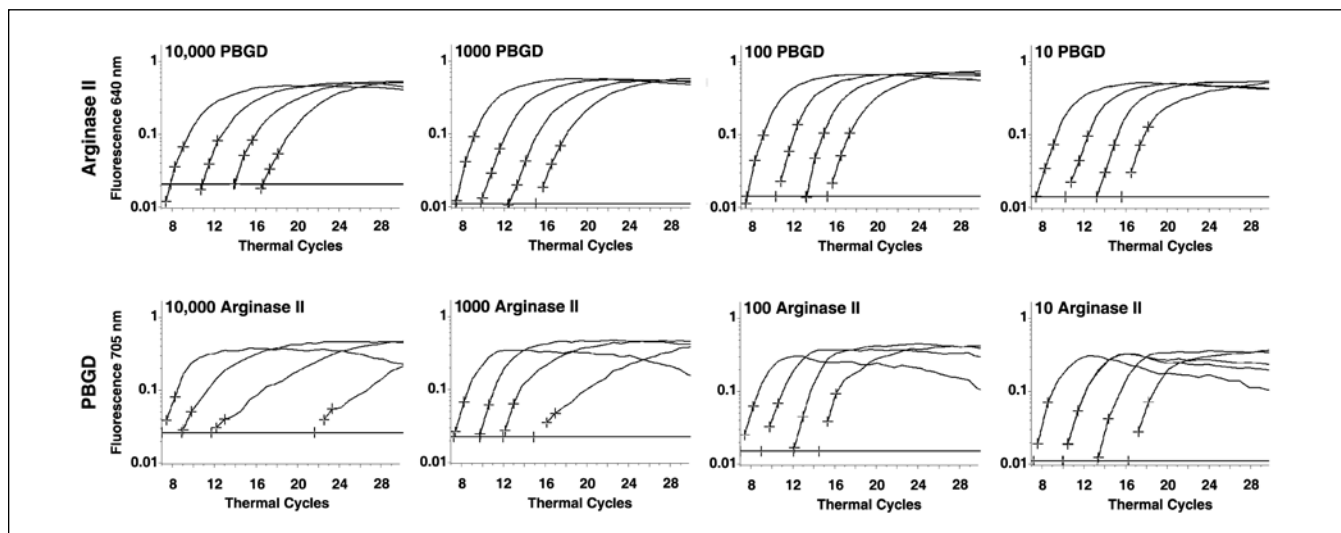


**Figure 1. The relative copy number of each target affects real-time duplex PCR amplification of arginase II and porphobilinogen deaminase (PBGD) standards.** To evaluate the performance of the duplex PCR standard at different target ratios and concentrations, a matrix of reactions (standard performance) was performed in which  $10^4$ ,  $10^3$ ,  $10^2$ , or 10 copies per reaction of the arginase II template were combined with  $10^4$ ,  $10^3$ ,  $10^2$ , or 10 copies of the PBGD template. Upper row: fluorescent signals for (left curve)  $10^4$ ,  $10^3$ ,  $10^2$ , and (right curve) 10 copies of the arginase II template at simultaneous amplification of  $10^4$ ,  $10^3$ ,  $10^2$ , or 10 copies of PBGD; lower row: signals for  $10^4$ –10 copies of the PBGD template at simultaneous amplification of  $10^4$ –10 copies of arginase II. Thermal cycling is calibrated to maximize the amplification efficiency of the arginase II analyte target at high or low PBGD copy numbers. Conversely, low copy numbers of the PBGD housekeeping gene target amplify poorly in the presence of high numbers of arginase II templates. This approach ensures valid results at low arginase II transcript levels. The highest sensitivity for the detection of housekeeping gene mRNA is not required because results by definition are inaccurate below 20 copies of the reference housekeeping gene mRNA.

spillover during the analysis of the results of duplex PCRs.

During attempts to combine the arginase I analyte target with the PBGD housekeeping gene target in a duplex PCR, we noticed extensive increases in the PBGD fluorescent signal at 705 nm emission wavelength at 10-fold or higher copy ratios of arginase I to PBGD standards (Figure 3). To evaluate if this excessive signal resulted from fluorescent spillover from the 640-nm arginase I emission peak, we removed either the BODIPY 630/650-labeled arginase I FRET acceptor probe or the Cy5.5-labeled PBGD FRET acceptor

probe from the duplex PCR. Removal of the PBGD probe, but not of the arginase I probe, eliminated the excessive signal in the PBGD emission channel. These data proved unequivocally that the excessive signal at 705 nm was not caused by a lack of compensation of fluorescence spillover but was generated directly by the PBGD Cy5.5-labeled FRET acceptor probe.

The minimum combination of reaction components necessary to create the aberrant PBGD signal were arginase I template, arginase I and PBGD primers, the Cy5.5-labeled PBGD probe, and either the arginase I or the PBGD

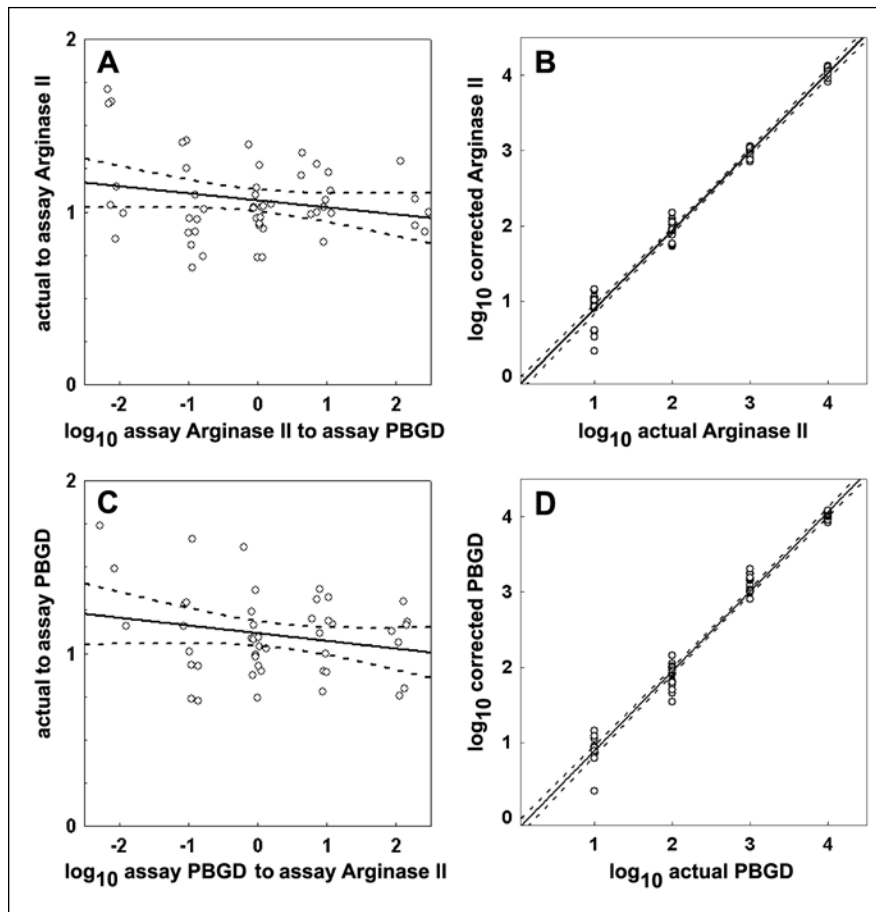


**Figure 2. Factors deduced from the standard performance reactions effectively correct the assay data of arginase II and porphobilinogen deaminase (PBGD).** Paired arginase II-PBGD data from four standard performance reactions (as shown in Figure 1) were used to evaluate the amplification of both targets relative to the known concentration of each standard. Least-square regression analysis obtained for each target a linear equation describing the relation between the logarithm of arginase II to PBGD copy numbers (and inverse ratio) and actual (true) copies divided by copies as determined in the assay (assay copies). The factor actual to assay copies is required for the correction of assay copies to the true number of target copies depending on the number of copies of the other respective target. The regression equation deduced in plot A (actual to assay arginase II =  $1.066 - 0.0408 \times \log_{10}$  assay arginase II to assay PBGD) was used to calculate correction factors for each pair of data from each sample in plot B. Assay PBGD data in plot D were corrected using the regression equation (actual to assay PBGD =  $1.1143 - 0.0494 \times \log_{10}$  assay PBGD to assay arginase II) deduced in plot C.

fluorescein probe. These reactions were analyzed by agarose gel electrophoresis, sequence alignments of the arginase I DNA fragment with primers and probes, and DNA sequencing (data not shown). A 146-bp product was identified in addition to the 212-bp arginase I fragment. Only the presence of large amounts of the arginase I fragment was associated with the production of this aberrant fragment. This 146-bp fragment was primed at the 5' end by the downstream PBGD primer (17 bp match) and downstream by the upstream PBGD primer (10 bp match) or downstream arginase I primer, resulting in a nested PCR from the original arginase I amplification product. Both the PBGD Cy5.5 and fluorescein probes match both the sense and antisense strands with 13–15 bp. Annealing of both PBGD probes to the noncoding

strand creates the thermodynamically most stable hybrids and separates the fluorescein and Cy5.5 labels by 3 bp. If the arginase I fluorescein probe is combined with the PBGD Cy5.5 probe, the fluorescent labels are separated by 23 bp on the noncoding strand. Both combinations of the PBGD Cy5.5 probe are sufficient to generate a 705-nm FRET signal under the conditions described. Thus, the muPBDGCY5.5 probe, annealing to high numbers of regular and aberrant arginase I amplification fragments in the arginase I-PBGD duplex PCR, interacted with both arginase I and PBGD fluorescein probes to produce excessive PBGD signal. Therefore, the coamplification of arginase I and PBGD targets in a duplex PCR was not compatible.

Subsequent removal experiments of all probes in the duplex PCRs described here revealed that fluorescent signals of the appropriate emission channels and target quantification did not differ in the reactions from PCRs performed with the complete set of probes. In addition, equations deduced from standard performance reactions of these reactions as well as for the arginase I signal in the arginase I-PBGD duplex PCR closely resembled those deduced here for both arginase II-PBDG duplex PCR channels (Figure 3). Therefore, electronic color compensation reliably and quantitatively corrected fluorescence spillover, and excessive signal such as that observed in the arginase I-PBGD duplex PCR was the result of sequence-specific interactions between the DNA targets and probes. Also, relative overreporting and underreporting in dependence on target ratios in standard performance reflected intrinsic properties of PCR assay chemistry, presumably competition between targets for rate-limiting *Taq* DNA polymerase, rather than insufficient electronic signal correction.

### Reproducibility of One-Step Real-Time Duplex RT-PCR

To assess the reproducibility

and accuracy of the established duplex RT-PCR methods over a range of target concentrations and ratios, we analyzed serial dilutions of total nucleic acid samples from *C. pneumoniae*-stimulated murine peritoneal macrophages. The raw numbers of mRNA copies of each target determined for two samples in both duplex RT-PCRs were multiplied with the appropriate correction factors, and copies of analyte mRNA were expressed as normalized copy numbers per 1000 copies of the respective housekeeping gene mRNAs. The corrected copy numbers of HPRT and PBGD mRNAs per 5  $\mu$ L of the undiluted samples were approximately 3000 and 1200, respectively. The results in Figure 4 indicate that the transcript levels of both arginase I and arginase II relative to HPRT and PBGD, respectively, remain nearly constant over a 64-fold range of sample nucleic acid concentrations. The increased standard deviation of analyte gene mRNAs per 1000 housekeeping gene mRNA in proportion to sample dilution indicates reduced accuracy at low copy numbers. The results of this analysis validate the reproducibility of both one-step real-time duplex RT-PCR methods within the range of target mRNA concentrations (10–10,000 copies/5  $\mu$ L) and ratios ( $10^{-2.5}$ – $10^{2.5}$ ; equal to 1/320 to 320) established in the standard performance reactions.

### DISCUSSION

The present study utilized Light-Cycler real-time PCR chemistry and step-down thermal cycling strategies developed previously (7,14) and adapted these methods to one-step reverse transcription, high-sensitivity amplification, and simultaneous real-time detection of two mRNA targets. This method provides several advantages over alternative approaches for mRNA quantification by real-time PCR (1,2). Most importantly, it simultaneously quantifies a target transcript of specific interest together with a second mRNA, typically an internal control mRNA of an essential gene present in all somatic cells in approximately constant steady-state equilibrium (4,5). Thus, one-step real-time duplex RT-PCR generates

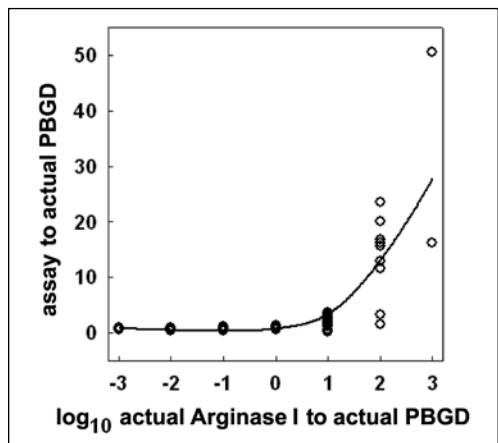


**Figure 3. Arginase I templates interact with the porphobilinogen deaminase (PBGD) Cy5.5 probe to produce an excessive PBGD signal at high arginase I-PBGD template ratios.** During method development, arginase I-PBGD duplex PCRs showed very high PBGD signals, resulting in PBGD overreporting when a 10-fold or higher excess of arginase I templates over PBGD templates was added to the reactions. The omission of the BODIPY 630/650-labeled arginase I probe from the duplex PCR did not eliminate this signal, but the removal of the Cy5.5-labeled PBGD probe did. The minimum reaction components necessary to create the aberrant PBGD signal were the combined arginase I template, arginase I and PBGD primers, the Cy5.5-labeled PBGD probe, and either the arginase I or the PBGD fluorescein probe. Subsequent analyses revealed that the muPBGDDN probe primed a 146-bp nested PCR fragment from large amounts of the original arginase I fragment. Both PBGD probes, or the arginase I fluorescein probe and the PBGD Cy5.5 probe, form thermodynamically sufficiently stable hybrids with the noncoding strand, separating the fluorescein and Cy5.5 labels by 3 or 23 bp, respectively. This resulted in the aberrant 705-nm fluorescence resonance energy transfer (FRET) signal, which made the coamplification of arginase I and PBGD targets in a duplex PCR incompatible.

results that allow for the calculation of the copy numbers of a target transcript in relation to a constant number of internal control transcripts of a housekeeping gene from the data of a single assay (normalization to relative quantification). This approach reduces inaccuracies such as differences in PCR efficiencies that cannot be avoided in methods that separate mRNA quantification into reverse transcription and single target amplifications. Furthermore, reverse transcription in one-step real-time duplex RT-PCR is primed by a gene-specific primer that also primes in PCR, which likely improves the efficiency of the production of target-length cDNA over reverse transcription that uses random oligonucleotide or oligo(dT) primers. Finally, the obvious simplicity of the one-step method will probably translate into enhanced precision by minimizing the number of experimental steps and sample transfers.

Additional advantages stem from

the choice of exon-spanning primers and probes that prevent the amplification or detection of genomic DNA. This approach allows PCR quantification of mRNA in total nucleic acid specimens and eliminates the need for the DNase treatment of RNA samples and controls necessary to assure amplification of cDNA but not of genomic DNA (1). The one-step real-time duplex RT-PCR methods in this study minimally detect 10 copies of analyte cDNA. However, our unpublished data of limiting standard and sample dilutions suggest that well-calibrated one-step real-time duplex RT-PCRs will detect a single copy of analyte cDNA in the presence of 20–30 copies of housekeeping gene cDNA. Thus, by virtue of the sensitive quantification of mRNAs in minute specimen volumes in a single assay, the greatest benefits of the one-step real-time duplex RT-PCR will most likely apply to clinical specimens. Such specimens typically provide limited

amounts of extracted total nucleic acids that are subjected to numerous analyses and might contain low concentrations of mRNA (15–17).

The appropriate choice of quantitative and qualitative positive and negative standards for one-step real-time duplex RT-PCRs is critical. Reactions of standard dilution buffer without target fragments, with and without reverse transcription, serve as negative amplification controls. In our hands, control for reverse transcription was best provided by known positive specimens. For quantitative determination, the interaction between the targets in duplex RT-PCRs during amplification and fluorescent signal detection is an important consideration. The matrix of standard performance reactions validates the method and determines equations for correction factors. Quantitative standards in the approach described in this study contain equal numbers of both double-stranded target

---

DNA fragments, not RNA standards, and are amplified without reverse transcriptase. The number of standard molecules is therefore absolute, not created by variable-rate reverse transcription of RNA standards. Reverse transcriptase generates sample cDNA but also reduces PCR efficiency by creating variable amounts of background DNA. Therefore, this approach relates target quantification in samples that are variable in their PCR inhibition to absolute target standards without reverse transcriptase-mediated inhibition. Background inhibition in duplex RT-PCR of unknown specimens affects the amplification of both targets. Therefore, analyte mRNA quantification relative to housekeeping gene mRNA remains unaffected by variable background PCR inhibition in specimens. Because

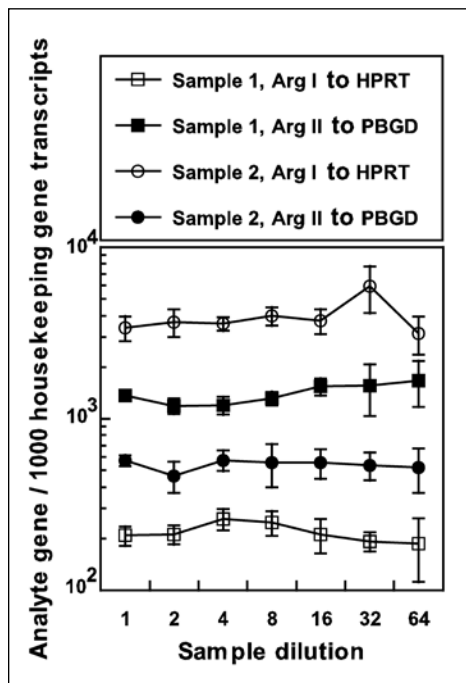


**Figure 4. Relative copy numbers of analyte and housekeeping genes in one-step real-time duplex RT-PCRs remain constant in assays of sample dilutions.** To test the overall performance of real-time duplex reverse transcription PCRs (RT-PCRs), quadruplicates of undiluted (1:1) and serial (1:2) dilutions of two total nucleic acid specimens from *Chlamydia pneumoniae*-stimulated murine macrophages were amplified for arginase I and hypoxanthine-phosphoribosyl transferase (HPRT) and arginase II and porphobilinogen deaminase (PBGD) mRNAs. Data are represented as the mean ( $\pm$  SD). The results indicate that the ratios of analyte to housekeeping mRNAs as determined by real-time duplex RT-PCR remain nearly constant over a 64-fold range of specimen nucleic acid concentrations. Arg I, arginase I; Arg II, arginase II.

of the PCR inhibitory background created by reverse transcription, careful calibration of each batch of reverse transcriptase is very important for the overall performance of one-step real-time duplex RT-PCRs.

The acceptable range of 1/320 to 320-fold ( $10^{-2.5}$ – $10^{2.5}$ ) target ratios in duplex RT-PCR specifies the limits of the analytical range of a real-time duplex RT-PCR. In essence, mRNA levels of analyte and housekeeping genes must be similar, and transcription levels of analytic targets will dictate the choice of housekeeping gene. In this study, we sought to use housekeeping genes with low transcription levels for the appropriate evaluation of genes typically transcribed at low levels. Additional housekeeping genes will be needed for duplex RT-PCRs deter-

mining high-concentration analyte mRNAs (4,5). Amplification fragments in such duplex PCR methods should be between 100–200 bp in length, and the  $T_m$  of primers and probes should be as high as 74°C to allow for highly stringent thermal-cycling conditions. Duplex RT-PCRs designed according to these guidelines can be conveniently established by first fine-tuning step-down cycling in 2°C annealing temperature steps starting approximately at the primer  $T_m$ , such that a signal for  $10^4$  target copies appears between cycles 6–8 of the subsequent fluorescence acquisition cycles. During these cycles, the 8-s fluorescence acquisition step at 58°C is critical and should not be modified. The omission of this step and fluorescence acquisition at higher temperature results in delayed but steep increases of the fluorescent signal over only 2–3 cycles from threshold to saturation signal, vastly reducing PCR accuracy. The efficiency of fluorescence acquisition cycles can be calibrated by adjusting the annealing temperature following fluorescence acquisition to a temperature between 61°–67°C. Quantification of more than  $10^4$  target copies is less challenging, and the total number of step-down cycles must be reduced by 3–4 cycles for each 10-fold increase of expected targets or the

specimen be appropriately diluted so that less than  $10^4$  target copies are present per PCR.

In summary, we have established sensitive real-time PCR methodology for the accurate quantification of eukaryotic analyte mRNA relative to a housekeeping gene in a single assay. The overall method discriminates cDNA from genomic DNA sequences and entails reverse transcription of both target mRNAs from total nucleic acids, followed by PCR amplification, real-time signal detection and quantification, and correction of assay results by factors deduced from reactions that evaluate quantification at variable ratios of the target standards. We have used this approach to develop, with ease, more duplex PCRs quantifying analyte mRNAs relative to PBGD and HPRT as well as additional housekeeping gene transcripts. We anticipate that one-step real-time duplex RT-PCR methods will accelerate the functional analysis of clinical specimens for gene transcription in the context of disease.

#### ACKNOWLEDGMENTS

*This study was supported by grants to B.K. from the United States Public Health Service (National Institutes of Health grant no. R01 AI 47202) (Washington, D.C.) and ActivBiotics (Lexington, MA).*

#### REFERENCES

1. **Bustin, S.A.** 2000. Absolute quantification of mRNA using real-time reverse transcription polymerase chain reaction assays. *J. Mol. Endocrinol.* 25:169-193.
2. **Bustin, S.A.** 2002. Quantification of mRNA using real-time reverse transcription PCR (RT-PCR): trends and problems. *J. Mol. Endocrinol.* 29:23-29.
3. **Kuhne, B.S. and P. Oschmann.** 2002. Quantitative real-time RT-PCR using hybridization probes and imported standard curves for cytokine gene expression analysis. *BioTechniques* 33:1078-1089.
4. **Thellin, O., W. Zorzi, B. Lakaye, B.D. Borman, B. Coumans, G. Hennen, T. Grislar, A. Igout, et al.** 1999. Housekeeping genes as internal standards: use and limits. *J. Biotechnol.* 75:291-295.
5. **Vandesompele, J., K.D. Preter, F. Pattyn, B. Poppe, N.Y. Roy, A.D. Paepe, and F. Spelman.** 2002. Accurate normalization of real-time quantitative RT-PCR data by geometric

- averaging of multiple internal control genes. *Genome Biol.* 3:research0034.1-0034.11.
6. **Huang, J., F.J. DeGraves, S.D. Lenz, D. Gao, P. Feng, D. Li, and B. Kaltenboeck.** 2002. The quantity of nitric oxide released by macrophages regulates *Chlamydia*-induced disease. *Proc. Natl. Acad. Sci. USA* 99:3914-3919.
7. **DeGraves, F.J., D. Gao, and B. Kaltenboeck.** 2003. High-sensitivity quantitative PCR platform. *BioTechniques* 34:106-115.
8. **von Ahsen, N., M. Oellerich, and E. Schutz.** 2000. A method for homogeneous color-compensated genotyping of factor V (G1691A) and methylenetetrahydrofolate reductase (C677T) mutations using real-time multiplex fluorescence PCR. *Clin. Biochem.* 33:535-539.
9. **Iyer, R.K., J.M. Bando, C.P. Jenkinson, J.G. Vockley, P.S. Kim, R.M. Kern, S.D. Cederbaum, and W.W. Grody.** 1998. Cloning and characterization of the mouse and rat type II arginase genes. *Mol. Genet. Metab.* 63:168-175.
10. **Shi, O., D. Kepka-Lenhart, S.M. Morris, Jr., and W.E. O'Brien.** 1998. Structure of the murine arginase II gene. *Mamm. Genome* 9:822-824.
11. **Strausberg, R.L., E.A. Feingold, L.H. Grouse, J.G. Derge, R.D. Klausner, F.S. Collins, L. Wagner, C.M. Shenmen, et al.** 2002. Generation and initial analysis of more than 15,000 full-length human and mouse cDNA sequences. *Proc. Natl. Acad. Sci. USA* 99:16899-16903.
12. **Beaumont, C., C. Porcher, C. Picat, Y. Nordmann, and B. Grandchamp.** 1989. The mouse porphobilinogen deaminase gene. Structural organization, sequence, and transcriptional analysis. *J. Biol. Chem.* 264:14829-14834.
13. **Melton, D.W., D.S. Konecki, J. Brennand, and C.T. Caskey.** 1984. Structure, expression, and mutation of the hypoxanthine phosphoribosyltransferase gene. *Proc Natl. Acad. Sci. USA* 81:2147-2151.
14. **Huang, J., F.J. DeGraves, D. Gao, T. Schlapp, and B. Kaltenboeck.** 2001. Quantitative detection of *Chlamydia* spp. by fluorescent PCR in the LightCycler®. *BioTechniques* 30:150-157.
15. **Culp, TD. and N.D. Christensen.** 2003. Quantitative RT-PCR assay for HPV infection in cultured cells. *J. Virol. Methods* 111:135-144.
16. **Huber, R., E. Kunisch, B. Gluck, R. Egerer, S. Sickinger, and R.W. Kinne.** 2003. Comparison of conventional and real-time RT-PCR for the quantitation of jun protooncogene mRNA and analysis of junB mRNA expression in synovial membranes and isolated synovial fibroblasts from rheumatoid arthritis patients. *Zeitschrift für Rheumatologie* 62:378-389.
17. **Smith A.B., V. Mock, R. Melear, P. Colarusso, and D.E. Willis.** 2003. Rapid detection of influenza A and B viruses in clinical specimens by LightCycler® real time RT-PCR. *J. Clin. Virol.* 28:51-58.

Received 14 September 2003; accepted 18 December 2003.

**Address correspondence to:**

Bernhard Kaltenboeck  
Department of Pathobiology  
College of Veterinary Medicine  
Auburn University  
270 Greene Hall  
Auburn, AL 36849-5519, USA  
e-mail: kaltebe@auburn.edu